의학박사 학위논문

Suture tie-down forces and cyclic contractile forces after an undersized tricuspid annuloplasty using a 3-dimensional rigid ring in an ovine model

양 모델에서 삼첨판막륜 축소 성형술 시행 시 부위별 고정 봉합 강도와 심장 수축 주기에 따른 부위별 봉합 강도의 측정

2021년 8월

서울대학교 대학원
의학과 흉부외과학 전공

임재홍

Suture tie-down forces and cyclic contractile forces after an undersized tricuspid annuloplasty using a 3-dimensional rigid ring in an ovine model

지도 교수 황 호 영

이 논문을 의학박사 학위논문으로 제출함
2021년 4월

서울대학교 대학원
의과대학 의학과 흉부외과학
임 재 홍

임재홍 의 의학박사 학위논문을 인준함
2021년 7월

위 원 장 김 웅 한

부위원장 황 호 영

위 원 임 청

위 원 김 기 범

위 원 박 진 수

Abstract

Objective

This study was conducted to measure suture tie-down forces and evaluate cyclic contractile forces (CCFs) in beating hearts after undersized 3-dimensional (3D) rigid-ring tricuspid valve annuloplasty (TAP).

Methods

Eight force transducers were attached to the 3D rigid TAP ring. Segment 1 to 8 were attached from the mid-septal to anterior-septal commissural area in a counterclockwise order. Two-sizes-down TAPs were performed in 6 sheep. Tie-down forces and CCF were recorded an analysed at the 8 annular segments and at 3 levels of peak right ventricular pressure (RVP: 30,50 and 70mmHg).

Results

The overall average tie-down forces and CCF were 4.34 ± 2.26 newtons (N) and 0.23 ± 0.09 N, respectively. The CCF at an RVP of 30mmHg were higher at 3 commissural areas (segment 3, 5 and 8) than at the other segments. The increases in th CCF following changes in the RVP were statistically significant only at the 3 commissural areas (P = 0.012). However, mean CCFs remained low at all annular positions (ranges of average CCF = 0.06-0.46 N).

Conclusions

The risk of suture dehiscence after down-sized 3D rigid-ring TAP might be minimal because the absolute forces remained low in all annular positions even in the condition of high RVP. However, careful suturing in the septal annular area and commissures in necessary to prevent an annular tear during a down-sized 3D ring-ring TAP.

* Part of this work has been published in European Journal of Thoracic and Cardiovascular Surgery (Jae Hong Lim et al. 2021 Mar 31. doi: 10.1093/ejcts/ezab131)

Keyword: Tricuspid valve, Tricuspid valve annuloplasty, Annuloplasty ring dehiscence

Student Number: 2012-21709

Table of Contents

List of tables and figures

List of Abbreviations

3D	3-dimensional
CCF	Cyclic contractile force
LMM	Linear mixed-effects model
RV	Right ventricle
RVP	Right ventricular pressure
TAP	Tricuspid valve annuloplasty
TR	Tricuspid regurgitation

Chapter 1. Introduction

1.1. Study Background

Tricuspid valve annuloplasty (TAP) is a preferred surgical procedure for patients with functional tricuspid regurgitation (TR). Previous studies have demonstrated that surgical outcomes of TAP using prosthetic rings are better than those of TAP using sutures in terms of T R recurrence [1−3]. Various rings have been introduced for TAP with pros and cons for each ring [4−7]. The 3-dimensional (3D) rigid ring (MC3 annuloplasty ring, Edwards Lifesciences, Irvine, CA, USA) is one such prosthetic ring that has exhibited favourable outcomes after TAP [5, 8, 9].

1.2. Purpose of Research

However, there is a concern that rigid rings pose a risk of ring dehiscence [10], which can occur while fixing the ring to the annulus or when the heart is beating after the ring is implanted. Previous study reported that rigid ring had 9-fold greater incidence of ring dehiscence than flexible ring and dehiscences were located at the septal annular area [10]. There was a study that measures of ovine tricuspid valve tissue strength with pull out test [11]. But there was no study about direct force measurement of tricuspid valve annulus during ring implantation and beating status after implantation. Therefore, this study was conducted to establish animal experiment model and measure suture tie-down forces during ring implantation and to evaluate cyclic contractile forces (CCFs) in beating hearts after undersized 3D

rigid ring TAP in an ovine model.

Chapter 2. Body

Materials and Methods

Experimental animals

Six 5-year-old male adult Corriedale sheep (57.3 ± 3.5 kg) were used in this study. Average life expectancy of sheep is 10 to 12 years. Normal sheep heart rate is 60 to 100 beats per minute and blood pressure is 90/60 mmHg to 120/80 mmHg. They received care in compliance with the protocols approved by the institutional animal care and use committee of our institution (approval number: 800-20180451) in accordance with human care guidelines.

Suture force transducers

A strain-gauge-based transducer was designed to isolate the tensile forces of the sutures. Two holes mounted in the transducer's frame allowed each device to be directly sutured to an annuloplasty ring to mimic a common ring annuloplasty technique. The apparatus consisted of 8 small 3D-printed specimens using a strain gauge (CEA-06-062UW-350, Vishay Micro-Measurements, Raleigh, NC, USA) to measure the strain at each location around the ring. At first, specimen was made of titanium. Titanium specimen was too hart to deform according to

right ventricular pressure (RVP). And then, specimen material was changed to polyamide plastic. Eight transducers were marked as segments 1 to 8: segments 1, 2 and 3 were placed at the septal annular area; segments 4 and 5, at the posterior annular area; and segments 6–8 at the anterior annular area (Figure 1). Dimensions and materials (HP 3D High Reusability PA 12, HP Development Company, L.P., Houston, TX, USA) of these specimens were selected to ensure that the force deformation would not cause any permanent damage to the apparatus. To calibrate the transducer, a customized force calibration device was designed (Figure 2). This device consisted of a force measurement sensor (DFS-BTA, Vernier, Beaverton, OR, USA), a linear actuator, a stepper motor (PKA544KD, Oriental Motor, Tokyo, Japan), and 5.6-inch industrial embedded computer (IEC 1000 Lite Series, HNS, Seoul, Korea), and a user interface that controlled the device (Figure 2). First, the specimen was fixed on a holder connected to the actuator using the same polyester suture material (2-0 Ethibond, Ethicon, Somerville, NJ, USA) used in the animal experiment. Second, as the linear actuator moved at a constant speed of 0.1 mm/s, specimen distances from the force sensor also increased because of the force applied to the specimen by increased suture tension. The strain and force data were acquired using the Data Acquisition (DAQ) device

NI9236 and USB6009 (National Instruments, Austin, T X, USA), followed by a LabView (National Instruments, Austin, TXU, SA)-based software program to save and monitor data. Thereafter, the recorded data were used to construct the linear calibration curve. Because the strain gauge was attached to the parts manually, every part was calibrated separately to obtain a precise force-strain calibration curve. Most difficult process of making transducers was electric wires attachment to signal sensor. At first, we just soldered electric wire to signal sensor. At that time, electric wires was too easy to detached from signal sensor. After several discussion, we overcame that problem with silicone glue (DOWSIL™ 3140 RTV Coating, DOW inc,, Midland, MI, USA).

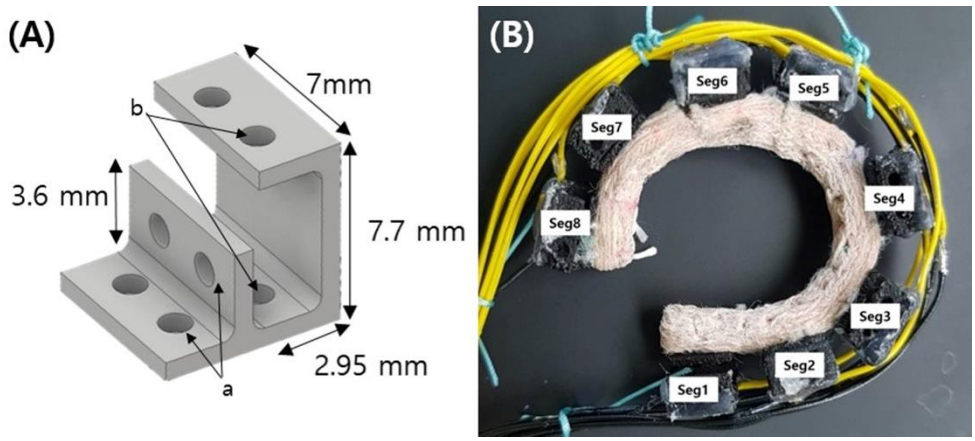

Figure 1. (A) A schematic of a transducer with (a) holes for a ring mounting and (b) mattress suture passages. (B) Complete transducer.

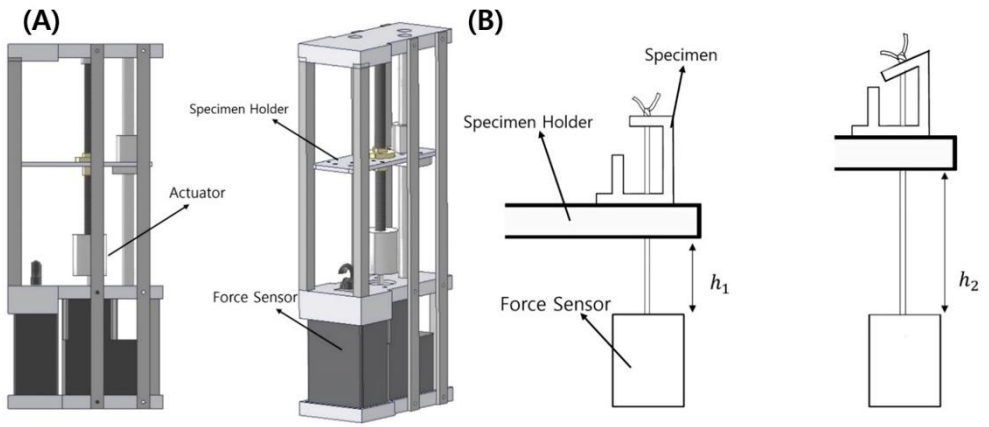

Figure 2. (A) The calibration device. (B) Schematic of the calibration procedure: the distance between the specimen and the force sensor differs because the holder moves at a constant velocity inducing the strain change.

In vivo experimental protocol

Each sheep was medicated with ketamine (25 mg/kg intramuscular injection), intubated and mechanically ventilated. General anaesthesia was induced with inhalational isoflurane (1.5–2%) and oxygen. The surface electrocardiogram and arterial blood pressure were monitored continuously during the experiment via right internal thoracic artery. The pericardial cavity was entered via a right thoracotomy at the level of scapula inferior tip, and cardiopulmonary bypass was established with systemic heparinization (Figure 3). The arterial cannula was placed in the right common carotid artery, and venous cannulae were inserted directly into the superior and inferior vena cavae and snared to prevent air trapping (Figure 3). After initiating cardioplegic arrest using the Custodiol histidine–tryptophan–ketoglutarate solution (Koehler–Chemie, Mensheim, Germany), a right atriotomy was performed. The actual annular size was measured using ring sizers, and a ring 2 sizes smaller than the measured size was selected for the experiment. Eight 2–0 polyester sutures were placed in the tricuspid annulus. The ring was implanted and secured using annular sutures through the mounting holes of the transducer measurement arms (Figure 4). Before the ring was lowered and secured into the tricuspid annulus, each transducer was zeroed to establish a zero–

force baseline. Annular mattress sutures were then tied to the ring by 1 surgeon from the mid-septal annulus to the anteroseptal commissure in a counterclockwise direction, and suture tie-down forces were recorded accordingly. After the animal was weaned from the cardiopulmonary bypass, 20 Fr intravenous catheter was inserted to right ventricular cavity directly and the right ventricular pressure (RVP) was continuously measured and monitored using a high fidelity pressure transducer. Continuous infusion and a bolus injection of an inotropic agent (epinephrine) were used to maintain a peak RVP of 30 mmHg, 50 mmHg and 70 mmHg for at least 30 s for each CCF measurement. Inotropic bolus injection was done via right atrium. When we injected to RV directly, frequent ventricular fibrillation was occurred. Then we changed right atrium injection, we solved that problem. The animal was then euthanized by injecting 80 mEq of potassium chloride. The heart was removed and opened to verify the secure anchoring of the device to the annulus. At second experiment, ovine ascending aorta was ruptured when we measured peak RVP 70mmHg because of aorta injury with crossclamp. Ovine aorta was more fragile than human's. Aorta crossclamp was changed to smoother one, after then aorta rupture was not occurred.

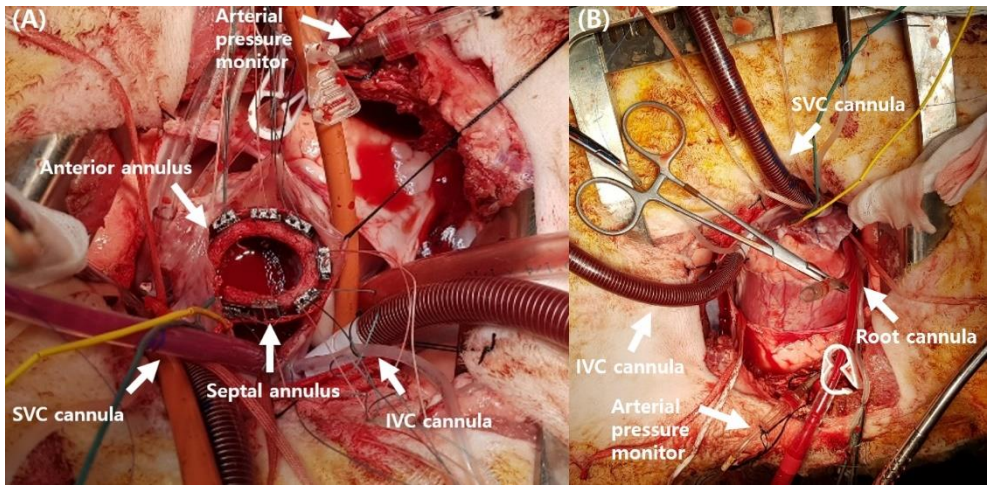

Figure 3. (A) Annuloplasty ring mounting to annulus, (B) After annuloplasty ring implantation

Figure 4. Illustration of ring implantation

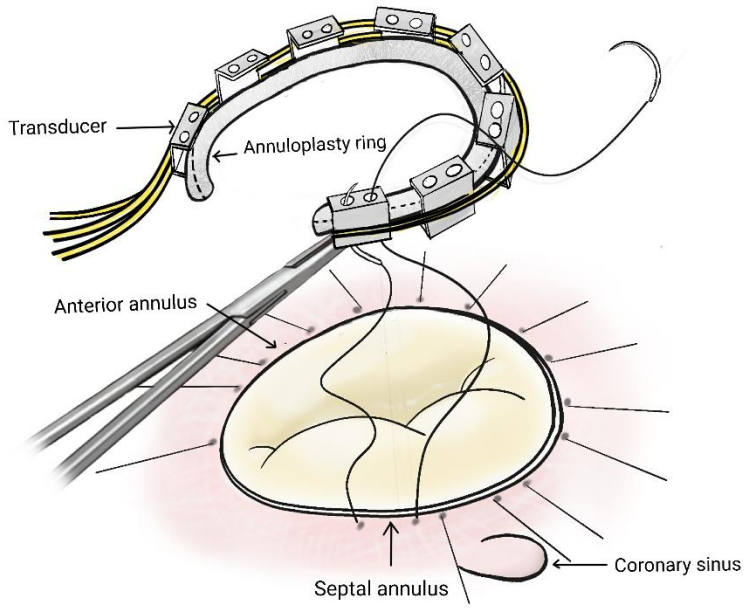

Data collection and analysis

During the experiment, the strain data were continuously acquired using the NI9236. From the data obtained, the maximum applied strain of each specimen was converted into a force by the designated calibrated curve in N units. To measure the average force applied to the specimens at different RVPs, the peaks and valleys of strain data due to heart contractions were detected by a customized code using the MAT LAB programme (MathWorks, Natick, MA, USA). The 20 successive strain differences obtained from the absolute difference between these peak and valley values were averaged for each specimen. These averaged strain values were then converted to force using the assigned calibration curve.

Statistical analyses

Statistical analyses were performed using the IBM SP SS statistic software version 23.0 (IBM Inc., Armonk, NY, USA) and SAS version 9.4 (SAS Institute, Cary, NC, USA). Force measurements were presented as means ± standard deviations. Mean differences in suture tie-down forces between segments and between annular areas were compared using the linear mixed-effects model (LMM), with segments and annular areas as fixed effects and each normal ovine variation as a random effect to account for multiple

measurements for each subject. An LMM with a random intercept was used because an LMM with a random intercept showed fit statistics (Akaike information criterion, Bayesian information criterion) similar to those of an LMM with a random intercept and a random segment.

To compare the means of the CCFs, the interaction between peak RVP and segments was assessed using an LMM. When the interaction was not significant, the mean differences among segments or segment groups and among peak RVPs were compared using the main effect results in an LMM without interaction terms. The mean estimates from a model with main effects only were similar to those from a model with main effects and interaction terms (Supplementary Material, Table S1).

The comparisons among segments or annular areas were each adjusted for peak RVP in an LMM. The comparison among peak RVPs was adjusted for segments in an LMM. The residual plots showed a random pattern, and their histograms revealed no severe violation of the normality assumption (Supplementary Material, Fig. S1A and B).

The Bonferroni adjusted *P*-value was used for multiple comparisons. Mean estimates and 95% confidence intervals for segments, segment groups and peak RVP from LMMs are

presented. A *P*-value of <0.050 was considered statistically significant.

Results

Ring selection and measurement of suture tie-down forces

A true tricuspid annulus measured 30 mm in all 6 sheep, and a 26-mm TAP ring was used in all experiments. Mean cardiopulmonary bypass and aortic cross-clamp times were 83 min and 54 min, respectively. The difference in suture tie-down forces was significant between segments ($P < 0.001$) (Table 1, Figure 5). The average suture tie-down force was 4.34 ± 2.26 N. The lowest suture tie-down force was 2.23 ± 0.53 N at the anteroposterior commissure (segment 5), whereas the highest force was 7.67 ± 2.33 N at the mid-septal annulus (segment 1). The septal annular area (segments 1-3, 6.22 ± 1.93 N) had significantly higher force than the posterior (segments 4 and 5, 2.87 ± 2.07 N) and anterior annular areas (segments 6-8, 3.45 ± 1.25 N) ($P < 0.001$; Table 2, Figure 5).

		P value
Segment 1	7.67 ± 2.33 N	< 0.001
Segment 2	5.54±1.36 N	–
Segment 3	5.45±1.24 N	–
Segment 4	3.52±2.86 N	–
Segment 5	2.23 ± 0.53 N	–
Segment 6	2.35±0.91 N	–
Segment 7	4.61±0.88 N	–
Segment 8	3.4±0.78 N	–
Septal (segments 1–3)	6.22±1.93 N	< 0.001
Posterior (segments 4, 5)	2.87±2.07 N	–
Anterior (segments, 6–8)	3.45±1.25 N	–
Total	4.34 ± 2.26 N	–

Table 1. Mean and standard deviation of suture tie-down forces in each segment and 3 annular areas.

N: newton, SD: standard deviation.

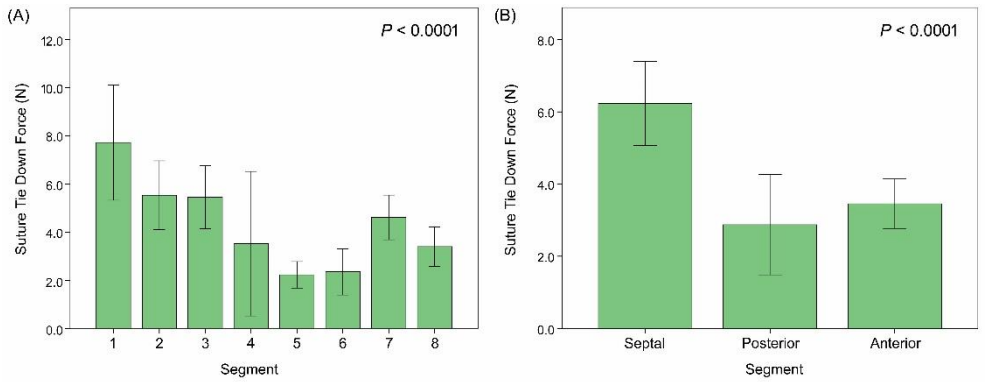

Figure 5. Suture tie-down force (A) at each position and (B) summation of forces at the septal, posterior and anterior annular areas. The force was significantly higher in the septal annular segments (6.22 ± 1.93 N) and lower at the posterior annular segments (2.87 ± 2.07 N; $P < 0.0001$). The bar graph depicts the mean and the 95% confidence interval of the suture tie-down force of each position and each annulus area.

Annular area	Differences of LSM (N)	95% CI	Adjusted p-value
Septal vs. posterior	3.345	2.031, 4.658	< 0.0001
Septal vs. anterior	2.765	1.589, 3.940	< 0.0001
Posterior vs. anterior	−0.580	−0.580, 0.733	> 0.9999

Table 2. Results of linear mixed effects model to compare suture tie-down forces between annulus

*values are presented as mean ± standard deviation

LSM, least square means; CI, confidence interval

Cyclic contractile force measurements

At each position, real-time forces exhibited strong coupling to RVP and low inter-cycle variability (Figure 6). Mean CCFs across all segments were 0.19 ± 0.17 N, 0.25 ± 0.16 N and 0.26 ± 0.21 N at the peak RVP of 30 mmHg, 50 mmHg and 70 mmHg, respectively. The CCFs were significantly different between segments ($P < 0.001$, Figure 7, Table 3), i.e. lowest at the posterior annular area (segments 4 and 5, 0.17 ± 0.09 N) and highest at the septal area (segments 1, 2 and 3, 0.30 ± 0.08 N). The CCF of 3 commissural areas (segments 3, 5 and 8) were different from each other ($P = 0.016$), and the posteroseptal commissure (segment 3) was highest among the 3 commissural areas ($P = 0.034$). The 3 commissural areas (segments 3, 5 and 8) had significantly higher CCF than other segments (0.27 ± 0.17 N vs 0.18 ± 0.18 N; $P = 0.009$) (Figure 7, Table 3).

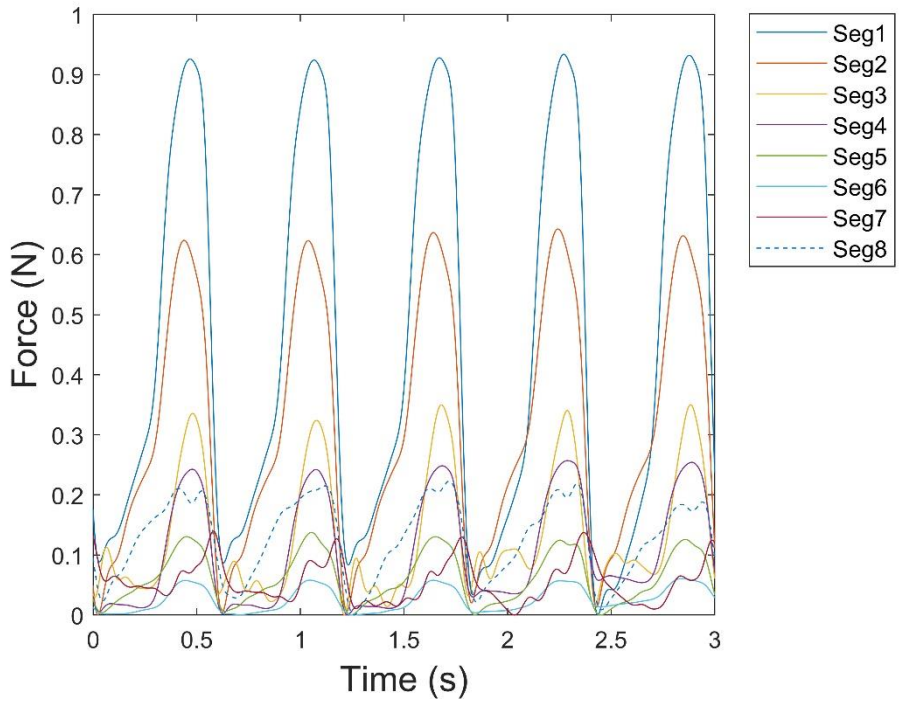

Figure 6. Representative figure of coupled recordings of cyclic contractile forces of 8 segments of the annuloplasty ring. Each trace corresponds to 1 mattress suture.

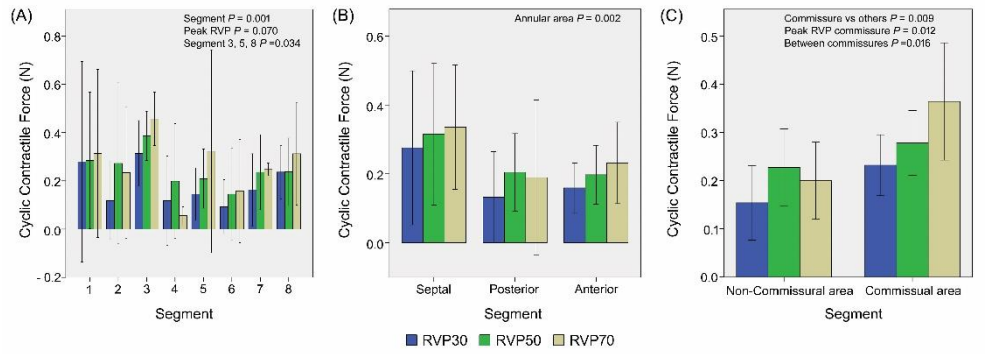

Figure 7. The cyclic contractile forces (CCF) in (A) each segment, (B) each annular area and (C) the commissural area at 3 levels (30mmHg, 50mmHg and 70mmHg) of RVP. Linear mixed-effects models demonstrated that the CCFs were significantly different between segments ($P < 0.001$). There was no significant difference in changes of the CCFs according to the RVPs ($P = 0.07$). The CCFs of each annular area were significantly different ($P = 0.002$). The CCF and CCF increases according to the changes in peak RVP were significantly higher at the 3 commissural areas (segments 3, 5 and 8) than the other segments ($P = 0.009$). Analysis of variance plots reported 95% confidence intervals of the influence of each suture position on CCFs.

RVP: right ventricular pressure.

	RVP = 30mmHg	RVP = 50mmHg	RVP = 70mmHg	Total	P value
Segment 1	0.28 ± 0.30 N	0.32±0.22 N	0.31 ± 0.28 N	0.31 ± 0.25	< 0.001[1]
Segment 2	0.21 ± 0.24 N	0.25 ± 0.25 N	0.23 ± 0.22 N	0.23 ± 0.22	
Segment 3	0.28 ± 0.13 N	0.35 ± 0.12 N	0.46 ± 0.09 N	0.36 ± 0.13	
Segment 4	0.11 ± 0.14 N	0.18 ± 0.18 N	0.06 ± 0.03 N	0.12 ± 0.14	
Segment 5	0.14 ± 0.08 N	0.23 ± 0.11 N	0.32 ± 0.34 N	0.23 ± 0.20	
Segment 6	0.10 ± 0.08 N	0.17 ± 0.15 N	0.16 ± 0.17 N	0.14 ± 0.13	
Segment 7	0.18 ± 0.09 N	0.26 ± 0.10 N	0.25 ± 0.02 N	0.23 ± 0.08	
Segment 8	0.22 ± 0.09 N	0.25 ± 0.11 N	0.31 ± 0.17 N	0.26 ± 0.12	
Septal (segments 1-3)	0.26 ± 0.22 N	0.31 ± 0.2 N	0.34 ± 0.22 N	0.30 ± 0.08 N	0.002[2]
Posterior (segments 4, 5)	0.12 ± 0.11 N	0.21 ± 0.14 N	0.19 ± 0.27 N	0.17 ± 0.09 N	
Anterior (segments 6-8)	0.16 ± 0.10 N	0.22 ± 0.12 N	0.24 ± 0.15 N	0.21 ± 0.12 N	
Commissural area (segment 3, 5, 8)	0.21 ± 0.11 N	0.28 ± 0.12 N	0.36 ± 0.22 N	0.27 ± 0.17 N	0.012[3]
Non-commissural area	0.17 ± 0.19 N	0.24 ± 0.18 N	0.20 ± 0.19 N	0.18 ± 0.18 N	0.009[4]
Total	0.19 ± 0.17 N	0.25 ± 0.16 N	0.26 ± 0.21 N		

Table 3. Cyclic contractile force (N) at 3 different levels of peak right ventricular pressure (RVP) in each segment and 3 annular area.

*values are presented as mean ± standard deviation

1. P value from overall F-test of segment in a linear mixed-effects model (LMM)
2. P value from overall F-test of annular areas in an LMM
3. P value from overall F-test of peak right ventricular pressure in a LMM
4. P value from overall F-test for comparison between commissural area vs other segments in a LMM

Discussion

This study demonstrated 3 main findings. First, the suture tie-down force at the septal annular area was significantly higher than those at the posterior and anterior annular areas. Second, the CCF was lowest at the posterior annular area and highest at the septal area. Third, the CCF was significantly higher in 3 commissural areas than those in the other segments with significantly increased CCF according to the increased peak RVP.

Various suture plication techniques and prosthetic TAP rings have been developed for the treatment of TR. The TAP rings have their own characteristics including hardness of the material and circumferential proportions in the tricuspid annulus. The design of the MC3 annuloplasty ring evaluated in this study was based on that of a 3D-shaped tricuspid annulus of a healthy heart and made as a rigid ring covering the annulus between the anteroseptal commissure to the mid-septal portion [12]. Previous studies have shown favourable results after TAP using this 3D ring [5, 8, 9]. Although the risk of dehiscence is still a concern when using the 3D rigid ring, objective data on this topic are limited. A previous study reported that early ring dehiscence causing severe TR occurred in 8 of 307 patients who received a rigid ring, and all of them were found in the septal annulus [10]. However, another study analysing

the holding strength of the suture with a pullout test in 15 ovine tricuspid annular tissues showed that the suture holding strength of the septal portion of the tricuspid annulus was greater than that of the other parts [11]. Tomasz et al. reported tricuspid valvular dynamics and 3-dimensional geometry in awake and anesthetized sheep [13]. They reported general anesthesia did not affected tricuspid annular and subvalvar geometry [13]. Also, there are some studies about TV dynamic changes during cardiac cycle of sheep before and after annuloplasty [14-16]. These studies revealed that annular dynamics were decreased after annuloplasty and rigid ring affected more than flexible ring [14-16]. In human study, the dynamic change in the septolateral diameter was lost in dilated RV [17]. Another study reported about tricuspid annular dynamics before and after annuloplasty [18]. They revealed flexible ring had greater dynamic diastolic to systolic change in anteroposterior and septolateral diameters than rigid ring but postoperative tricuspid valve regurgitation degree was not significantly different [18]. There are some study about mitral valve annular dynamics include animal experiment and human [19-22]. We were inspired by these studies. Rhomoto et al. reported physiological mitral annular dynamics after annuloplasty [20]. They reported rigid and semi-rigid ring could restore annular shape and

semi-flexible ring could preserve physiological annular dynamics in mid-term period [20].

In this study, down-sized ring annuloplasty was performed to mimic the daily practice for the treatment of functional TR, and CCFs were measured in various RVPs. There are various invasive or non-invasive parameters to access right ventricular (RV) function, including RV peak systolic pressure [23]. However, there is no satisfactory parameter to show exact RV function because of RV anatomical morphology. Therefore, we assumed that CCF measurements at various RVPs using inotropic infusion and injection can represent the situation created by the different contractility forces of the right ventricle. The average suture tie-down force of 4.34 N was higher than the values reported in a previous study that measured suture tie-down forces during mitral ring annuloplasty (2.9 N and 2.2 N for each surgeon), whereas the average CCF of 0.26 N at 70 mmHg RVP was lower than that after mitral annuloplasty (2.0 N) [22]. Individual surgeon variation might exist when tying down the sutures. However, in this study, suturing and knot-tying were performed by a single surgeon who was unaware of the purpose of measuring the tie-down forces during TAP, which was found to be significantly higher in the septal annulus than that in other parts.

CCFs were also higher in the septal area than those in the other annular parts. These findings agreed with those from a previous study that showed that suture dehiscence occurred exclusively in the septal annulus after a rigid-ring TAP [10].

Therefore, careful annular suturing and knot-tying might be needed, particularly in the septal annular segments, to prevent cut-through and early dehiscence of the ring when using a rigid TAP ring. In addition, this study showed that CCFs were greater at the commissural segments than at the leaflet midpoints. When considering the findings in a previous study [11] in *ex vivo* ovine pullout tests showing that the holding strength of the suture was weaker at the commissures than that at leaflet midpoints, suturing the commissural area should be carefully performed to prevent suture dehiscence in the commissural area.

Limitation

The present study some limitations. First, this study included healthy adult sheep, and the characteristics of the tricuspid annulus might be different from those of a human heart with functional TR. Development of diseased model may be needed for further study. Second, the number of study animals was relatively small even though this study demonstrated statistically significant findings.

Third, intraoperative echocardiographic evaluation was not performed, and the RV condition was controlled based on RV pressure rather than on RV function. Although weaning from cardiopulmonary bypass was successful in all the animals, and inotropic agents were used to maintain peak RV pressure, exact left ventricular and RV size and function could not be presented. Fourth, the ring was inserted in an arrested heart, which is a daily routine in our institution. However, our practice may differ from the practices of other institutions, and transient RV dysfunction after cardioplegic arrest could affect the study results.

Chapter 3. Conclusion

Conclusion

This is the first study about direct measure of tricuspid annular suture tie-down force and cyclic contractile force of beating heart and suggests that about tricuspid valve annuloplasty suturing skills and tie-down order. The risk of suture dehiscence after a down-sized 3D rigid-ring TAP might be low because absolute forces remained low in all annular positions, even in high RVP conditions. However, careful suturing is warranted at the septal annular area and commissures to prevent annular tear after the down-sized 3D rigid-ring TAP.

Bibliography

[1] Tang GH, David TE, Singh SK, Maganti MD, Armstrong S, Borger MA. *Tricuspid valve repair with an annuloplasty ring results in improved long-term outcomes*. Circulation 2006;114:I577-81.

[2] Guenther T, Mazzitelli D, Noebauer C, Hettich I, Tassani-Prell P, Voss B *et al. Tricuspid valve repair: is ring annuloplasty superior?* European journal of cardio-thoracic surgery : official journal of the European Association for Cardio-thoracic Surgery 2013;43:58-65; discussion 65.

[3] Parolari A, Barili F, Pilozzi A, Pacini D. *Ring or suture annuloplasty for tricuspid regurgitation? A meta-analysis review*. The Annals of thoracic surgery 2014;98:2255-63.

[4] Izutani H, Nakamura T, Kawachi K. *Flexible band versus rigid ring annuloplasty for functional tricuspid regurgitation*. Heart Int 2010;5:e13.

[5] Choi JW, Kim KH, Kim SH, Yeom SY, Hwang HY, Kim KB. *Long-Term Results of Tricuspid Annuloplasty Using MC3 Ring for Functional Tricuspid Regurgitation*. Circ J 2018;82:2358-63.

[6] Zhu TY, Wang JG, Meng X. *Is a rigid tricuspid annuloplasty ring superior to a flexible band when correcting secondary tricuspid regurgitation?* Interactive cardiovascular and thoracic surgery

2013;17:1009-14.

[7] Ratschiller T, Guenther T, Guenzinger R, Noebauer C, Kehl V, Gertler R *et al. Early experiences with a new three-dimensional annuloplasty ring for the treatment of functional tricuspid regurgitation*. The Annals of thoracic surgery 2014;98:2039-44.

[8] Yoda M, Tanabe H, Kadoma Y, Suma H. *Mid-term results of tricuspid annuloplasty using the MC3 ring for secondary tricuspid valve regurgitation*. Interactive cardiovascular and thoracic surgery 2011;13:7-10.

[9] Jeong DS, Kim KH. *Tricuspid annuloplasty using the MC3 ring for functional tricuspid regurgitation*. Circ J 2010;74:278-83.

[10] Pfannmuller B, Doenst T, Eberhardt K, Seeburger J, Borger MA, Mohr FW. *Increased risk of dehiscence after tricuspid valve repair with rigid annuloplasty rings*. J Thorac Cardiovasc Surg 2012;143:1050-5.

[11] Paul DM, Naran A, Pierce EL, Bloodworth CHt, Bolling SF, Yoganathan AP. *Suture Dehiscence in the Tricuspid Annulus: An Ex Vivo Analysis of Tissue Strength and Composition*. The Annals of thoracic surgery 2017;104:820-26.

[12] Filsoufi F, Salzberg SP, Coutu M, Adams DH. *A three-dimensional ring annuloplasty for the treatment of tricuspid regurgitation*. The Annals of thoracic surgery 2006;81:2273-7.

[13] Jazwiec T, Malinowski M, Proudfoot AG, Eberhart L, Langholz D, Schubert H, et al. Tricuspid valvular dynamics and 3-dimensional geometry in awake and anesthetized sheep. J Thorac Cardiovasc Surg 2018;156:1503-1511.

[14] Jazwiec T, Malinowski M, Ferguson H, Wodarek J, Quay N, Bush J, et al. Effect of variable annular reduction on functional tricuspid regurgitation and right ventricular dynamics in an ovine model of tachycardia-induced cardiomyopathy. J Thorac Cardiovasc Surg 2021;161:e277-e286.

[15] Malinowski M, Jazwiec T, Quay N, Goehler M, Rausch MK, Timek TA. The influence of tricuspid annuloplasty prostheses on ovine annular geometry and kinematics. J Thorac Cardiovasc Surg 2021;161:e191-207.

[16] Malinowski M, Schubert H, Wodarek J, Ferguson H, Eberhart L, Langholz D, et al. Tricuspid Annular Geometry and Strain After Suture Annuloplasty in Acute Ovine Right Heart Failure. The Annals of thoracic surgery 2018;106:1804-1811.

[17] Ring L, Rana BS, Kydd A, Boyd J, Parker K, Rusk RA. Dynamics of the tricuspid valve annulus in normal and dilated right hearts: a three-dimensional transoesophageal echocardiography study. Eur Heart J Cardiovasc Imaging 2012;13:756-762

[18] Nishi H, Toda K, Miyagawa S, Yoshikawa Y, Fukushima S,

Kawamura M, et al. Tricuspid annular dynamics before and after tricuspid annuloplasty- three-dimensional transesophageal echocardiography. Circ J 2015;79:873-879.

[19] Rausch MK, Bothe W, Kvitting JP, Swanson JC, Ingels NB, Jr., Miller DC, et al. Characterization of mitral valve annular dynamics in the beating heart. Annals of biomedical engineering 2011;39: 1690-1702.

[20] Ryomoto M, Mitsuno M, Yamamura M, Tanaka H, Sekiya N, Uemura H, et al. Physiological mitral annular dynamics preserved after ring annuloplasty in mid-term period. Gen Thorac Cardiovasc Surg 2017;65: 627-632.

[21] van Wijngaarden SE, Kamperidis V, Regeer MV, Palmen M, Schalij MJ, Klautz RJ, et al. Three-dimensional assessment of mitral valve annulus dynamics and impact on quantification of mitral regurgitation. Eur Heart J Cardiovasc Imaging 2018;19:176-184.

[22] Pierce EL, Bloodworth CHt, Siefert AW, Easley TF, Takayama T, Kawamura T *et al. Mitral annuloplasty ring suture forces: Impact of surgeon, ring, and use conditions*. J Thorac Cardiovasc Surg 2018;155:131-39 e3.

[23] Sanz J, Sanchez-Quintana D, Bossone E, Bogaard HJ, Naeije R. *Anatomy, Function, and Dysfunction of the Right Ventricle: JACC State-of-the-Art Review*. J Am Coll Cardiol 2019;73:1463-82.

Supplementary materials

peak RVP	Segment	Mean estimate (95% CI)	
		Model with main effects	Model with main effects and their interaction terms
30mmHg	1	0.26 (0.16, 0.36)	0.28 (0.14, 0.42)
	2	0.19 (0.09, 0.28)	0.21 (0.07, 0.35)
	3	0.31 (0.22, 0.41)	0.28 (0.14, 0.42)
	4	0.07 (−0.02, 0.17)	0.11 (−0.04, 0.25)
	5	0.18 (0.09, 0.28)	0.14 (0.00, 0.28)
	6	0.10 (0.00, 0.19)	0.10 (−0.05, 0.24)
	7	0.17 (0.07, 0.27)	0.17 (0.01, 0.32)
	8	0.21 (0.12, 0.31)	0.22 (0.08, 0.36)
50mmHg	1	0.32 (0.23, 0.42)	0.32 (0.18, 0.46)
	2	0.25 (0.15, 0.34)	0.25 (0.11, 0.39)
	3	0.38 (0.28, 0.47)	0.35 (0.21, 0.49)
	4	0.14 (0.04, 0.23)	0.18 (0.04, 0.32)
	5	0.25 (0.15, 0.34)	0.23 (0.09, 0.38)
	6	0.16 (0.06, 0.26)	0.17 (0.03, 0.31)
	7	0.23 (0.13, 0.34)	0.25 (0.09, 0.40)
	8	0.28 (0.18, 0.37)	0.25 (0.11, 0.39)
70mmHg	1	0.33 (0.23, 0.43)	0.31 (0.16, 0.47)
	2	0.26 (0.16, 0.36)	0.23 (0.08, 0.39)
	3	0.39 (0.29, 0.48)	0.46 (0.30, 0.61)
	4	0.15 (0.05, 0.25)	0.05 (−0.10, 0.21)
	5	0.26 (0.16, 0.35)	0.32 (0.17, 0.48)
	6	0.17 (0.07, 0.27)	0.16 (0.00, 0.31)
	7	0.24 (0.14, 0.35)	0.23 (0.06, 0.40)
	8	0.29 (0.19, 0.39)	0.31 (0.16, 0.47)

Supplementary Table 1. The mean estimates from a model only with main effects and a model with main effects an interaction terms.

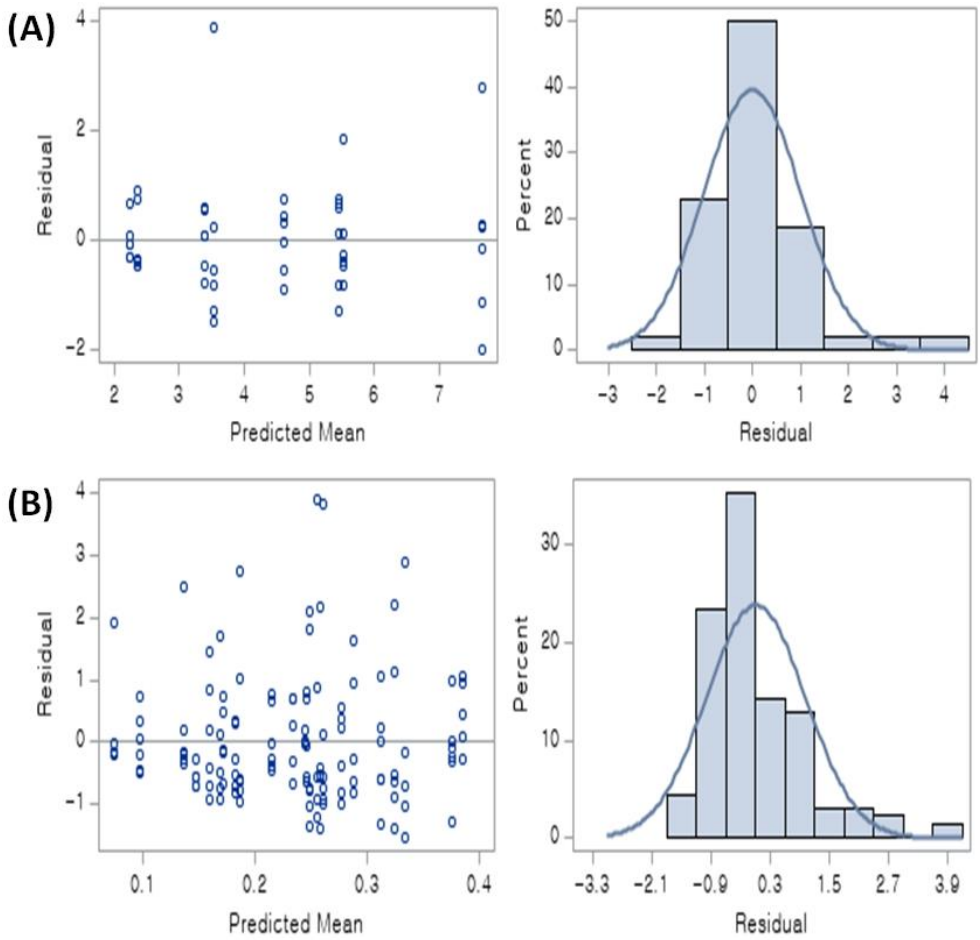

Supplementary Figure 1. Residual plots in the models for the suture tie-down force and cyclic contractile force (CCF). (A) Residual distribution of suture tie-down force, (B) Residual distribution of CCF.

국문 초록

목적

삼첨판막륜 축소 성형술 시행 시 고정 봉합 강도와 심장 수축 주기에 따른 부위별 봉합 강도의 측정을 위해 연구를 시행하였다.

방법

8개의 변환기를 3차원 삼첨판막 성형 링에 부착하였다. 1구간에서 8구간은 삼첨판막의 중격 판막륜 중간에서 시작하여 앞-중격 판막 연결부위까지 반 시계방향으로 부착하였다. 총 6마리의 양에 2크기 축소 링 삼첨판막륜 성형술을 시행하였다. 링의 8개 구간에서의 고정 봉합 강도와 우심실 압력 30, 50, 70mmHg에서의 심장 수축 주기에 따른 부위별 봉합 강도를 기록하고 분석하였다.

결과

고정 봉합 강도와 심장 수축 주기에 따른 봉합 강도는 3.34 ± 2.26 N, 0.23 ± 0.09 N 이었다. 심장 수축 주기에 따른 봉합 강도는 우심실 압력 30 mmHg일 때 각 판막의 연결 부위에서 다른 부위 보다 높았다(3, 5, 8 구간). 우심실 압력이 높아질 때 심장 수축 주기에 따른 봉합 강도는 각 판막의 연결 부위에서만 증가하였다 (P=0.012). 그러나 심장 수축 주기에 따른 봉합 강도의 평균은 모든 부위에서 낮았다 (평균 0.06-0.46 N).

결론

삼첨판막륜 축소 성형술 이후 링 열개의 위험도는 모든 부위에서의 절대적인 힘의 크기가 높은 우심실 압력에서도 작아서 낮을 수 있다. 그러나 삼첨판막륜 축소 성형술 시행 시 판막륜 찢어짐을 예방하기 위해 중격 판막 륜 부위와 각 판막의 연결 부위를 주의해서 봉합 할 필요가 있다.

주요어: 삼첨판막, 삼첨판막륜 성형술, 판막륜 성형 링 열개

학번: 2012-21709